ANIONIC SITES OF HUMAN ERYTHROCYTE MEMBRANES

I. Effects of Trypsin, Phospholipase C, and pH on the Topography of Bound Positively Charged Colloidal Particles

GARTH L. NICOLSON

From the Cancer Council and Electron Microscopy Laboratories, Armand Hammer Center for Cancer Biology, The Salk Institute for Biological Studies, San Diego, California 92112

ABSTRACT

The effects of pH, trypsin, and phospholipase C on the topographic distribution of acidic anionic residues on human erythrocytes was investigated using colloidal iron hydroxide labeling of mounted, fixed ghost membranes. After glutaraldehyde fixation at pH 6.5–7.5, the positively charged colloidal particles were bound to the membranes in small randomly distributed clusters. The clusters of anionic sites were reversibly aggregated by incubation at pH 5.5 before fixation at the same pH. These results correlate with the distribution of intramembranous particles found by Pinto da Silva (*J. Cell Biol.* **53**:777), with the exception that the distribution of anionic sites on a majority of the fixed ghosts at pH 4.5 was aggregated instead of dispersed. The randomly distributed clusters could be nonreversibly aggregated by trypsin or phospholipase C treatment of intact ghosts before glutaraldehyde fixation. Previous glutaraldehyde fixation prevented trypsin and pH induced aggregation of the colloidal iron sites. Evidence that *N*-acetylneuraminic acid groups are the principal acidic residues binding colloidal iron was the elimination of greater than 85% of the colloidal iron labeling to neuraminidase-treated cell membranes. Colloidal iron binding *N*-acetylneuraminic acid residues may reside on membrane molecules such as glycophorin, a sialoglycoprotein which contains the majority of the *N*-acetylneuraminic acid found on the human erythrocyte membrane.

INTRODUCTION

Human erythrocytes possess a large net negative surface charge at their electrokinetic surface under physiological conditions (1, 20, 44). This electrokinetic negative surface charge has been determined to be due mainly to acidic oligosaccharide anionic residues such as *N*-acetylneuraminic acid (NANA)[1] (11, 44, 49). It has been suggested that the surface distribution of acidic anionic residues on erythrocytes and other cells may be important in preventing (or allowing) cell-cell or cell-molecule interactions to occur in vivo, if changes in the local densities of acidic residues affect these interactions. For example, it is known that viral transformation changes the quantity of

[1] *The following abbreviations are used in this paper: CD*, circular dichroism; *CIH*, colloidal iron hydroxide; *NANA*, *N*-acetylneuraminic acid; *NANAse*, *N*-acetylneuraminic acid hydrolyase; *PLC*, phospholipase C; *Tris-HCl*, tris (hydroxymethyl)-aminomethane hydrochloride 300 *PB*, 0.05 M sodium phosphate, 0.6% sodium chloride buffer, pH 7.5, 300 mosmol.

plasma membrane NANA (28, 52), and Weiss has proposed that these changes may influence cell social behavior (44).

Currently the most popular electron microscope technique for localizing anionic residues on membrane surfaces is the colloidal iron hydroxide (CIH) method of Gasic et al. (12, 13). While developing techniques for elucidating topographical changes in cell surface components after neoplastic transformation (21, 23, 24), I adapted the Gasic CIH staining techniques to determine the two-dimensional distribution of acidic anionic residues on glutaraldehyde-fixed membrane ghosts (22). This was done by first mounting the intact, fixed ghosts onto thin support films. The flattened membranes were then stained with CIH at pH 1.8, dried, and finally observed by conventional transmission electron microscopy (22). Here the distributions of bound CIH on fixed human erythrocyte ghost membranes are compared after modifying the membranes by protease (trypsin), lipase (phospholipase C), or pH treatments.

MATERIALS AND METHODS

Glutaraldehyde was obtained from Union Carbide Corp. (New York) as a 50% solution and was fractionally distilled before use. Glacial acetic acid, ferric chloride, calcium chloride, sodium acetate, sodium chloride, and sodium phosphates were obtained as reagent grade materials from Mallinckrodt Chemical Works (St. Louis, Mo.). Tris(Hydroxymethyl)aminomethane hydrochloride (Tris-HCl) was obtained from Sigma Chemical Co. (St. Louis, Mo.).

Preparation of Erythrocyte Ghosts

Blood (B^+ or O^+) was collected in heparinized vacuum tubes (Becton-Dickinson & Co., Rutherford, N. J.) and washed several times in 0.9% NaCl. The white coat was aspirated after each centrifugation. The erythrocyte ghosts were prepared at 4°C by the method of Dodge et al. (9), except that sodium phosphate buffer, pH 7.4, 15 mosmol (15 PB) was used as the hemolyzing buffer. The lysed cells were washed 4–5 × in the hemolyzing buffer by centrifugation at 15,000 *g* for 10–15 min and finally resuspended in 0.05 M sodium phosphate-0.6% sodium chloride buffer, pH 7.4, 300 mosmol (300 PB) (23) and allowed to reseal for 15 min at 4°C. Some of the washed ghosts were fixed in 1.5% glutaraldehyde (sodium phosphate buffer, 300 mosmol, pH 7.4) for 30–60 min at room temperature and washed by centrifugation as before in 300 PB. Both fixed and unfixed erythrocyte ghosts at each step were examined by phase microscopy using a modified Vanox-Olympus Universal Microscope fitted with Zeiss optics (McBain Instruments, Van Nuys, Calif.).

pH Treatments of Erythrocyte Ghosts

Procedures generally follow those of Pinto da Silva (33). Unfixed ghosts were washed twice in 8 mM sodium phosphate, Tris·HCl, or sodium acetate (pH listed in Table I) containing additionally 0.5 mM calcium chloride. The washed ghosts were fixed at their respective pH by addition of 1.5% glutaraldehyde at room temperature. The pH was held constant for 30 min by titration and pH monitoring using a digital pH meter (Corning Model 110, Corning Scientific Instruments, Meldfield, Mass.). After fixation the ghosts were washed once in their respective buffers (Table I).

Enzyme Treatments of Erythrocyte Ghosts

Washed unfixed ghosts (0.2 ml pellet) in 300 PB or 15 PB at room temperature and at 37°C were incubated with 0.001% trypsin (crystallized, Worthington Biochemical Corp., Freehold, N. J.) for 30 min. At that time a 10-fold excess of ovomucoid (crystallized, Sigma Chemical Co.) was added and the trypsinized ghosts were washed twice (as before) in buffer and fixed for 30 min in 1.5% glutaraldehyde followed by an additional buffer wash.

Neuraminidase treatment was as follows: washed unfixed ghosts (0.2 ml pellet) were incubated in 0.02 M Tris-maleate-0.85% NaCl buffer, pH 5.5, containing 250 U *Vibrio cholerae* neuraminidase (NANAse) (Calbiochem, San Diego, Calif.) for 30 min at 37°C. This treatment cleaved greater than 90% of the membrane NANA as determined by the method of Warren (43). The NANAse-treated ghosts were washed twice in 300 PB and fixed for 30–60 min in 1.5% glutaraldehyde, as above.

Phospholipase C (PLC) treatment was performed with a partially purified *Cl. perfringens* preparation (Worthington Biochemical Corp.) that was protease-freed according to the procedures of Glaser et al. (14), and Simpkins et al. (35A), or a purified preparation from *B. cereus* (29). Unfixed ghosts (0.2 ml pellets) were washed twice in 0.01 M Tris-HCl, pH 7.4, and incubated with 1 mg/ml of the *Cl. perfringens* PLC or 0.05 mg/ml of the *B. cereus* preparation for 30 min at 37°C. These PLC incubations resulted in the liberation of 62–70% of the total membrane phosphorus (14, 17) determined by the method of Bartlett (2). The PLC-treated ghosts were washed twice in 300 PB and fixed in 1.5% glutaraldehyde, as above.

Colloidal Iron Hydroxide (CIH) Labeling

CIH was prepared according to a modification (22) of the procedures of Gasic et al. (13). 5 ml of

TABLE I

Human Erythrocyte Ghost Labeling Experiments

Experiment	First incubation			Second incubation			Ghost morphology§	Topography of CIH‖
	Buffer*	pH	Subsequent fixation‡	Buffer*	pH	Subsequent fixation‡		
pH	Tris	7.5	+				Smooth	Dispersed
	Phos	7.5	+				Smooth	Dispersed
	Phos	6.5	+				Smooth	Dispersed
	Phos	5.5	+				Crumpled	Aggregated
	Ac	5.5	+				Crumpled	Aggregated
	Phos	4.5	+				Rough/smooth¶	Aggreg/disp¶
	Ac	4.5	+				Rough/smooth¶	Aggreg/disp¶
	Phos	7.5	−	Phos	5.5	+	Crumpled	Aggregated
	Tris	7.5	−	Phos	5.5	+	Crumpled	Aggregated
	Phos	7.5	−	Ac	5.5	+	Crumpled	Aggregated
	Phos	7.5	−	Phos	4.5	+	Rough/smooth¶	Aggreg/disp¶
	Ac	5.5	−	Phos	7.5	+	Smooth	Dispersed
	Ac	5.5	−	Tris	7.5	+	Smooth	Dispersed
	Phos	4.5	−	Phos	7.5	+	Smooth	Dispersed
	Phos	7.5	+	Ac	5.5	−	Smooth	Dispersed
	Ac	5.5	+	Phos	7.5	−	Crumpled	Aggregated
	Phos	4.5	+	Phos	7.5	−	Rough/smooth¶	Aggreg/disp¶
Trypsin**	Phos	7.5	−	Phos + Tryp**	7.5	+	Smooth	Aggregated
	Phos	7.5	+	Phos + Tryp**	7.5	−	Smooth	Disp/aggreg‡‡
Phospholipase C§§	Tris	7.5	−	Tris + PLC§§	7.5	+	Smooth‖‖	Aggregated

* Abbreviations: Tris, 8 mM Tris-HCl; Phos, 8 mM sodium phosphate; Ac, 8 mM sodium acetate.

‡Glutaraldehyde fixation (1.5%) for 60 min at 20°C.

§ Ghost morphology determined by phase contrast microscopy (see Results).

‖ Topography of CIH particles on glutaraldehyde-fixed ghosts; Disp, dispersed CIH clusters; Aggreg, definite aggregation of CIH clusters.

¶ Both "smooth" and "rough" shaped ghosts were present having dispersed and aggregated CIH distributions, respectively.

** 0.001% trypsin for 30 min at 37°C.

‡‡ An overwhelming majority of the ghosts had dispersed distributions, but the total number of bound CIH particles was reduced.

§§ 0.001% *C. perfringens* phospholipase C or 0.0005% *B. cereus* phospholipase C for 30 min at 37°C.

‖‖ Phospholipase C treated ghosts were smooth shaped vesicles containing small globular appearing regions of high contrast ("blebs").

0.5 M $FeCl_3$ was added rapidly to 60 ml of boiling glass distilled water. After cooling, 10 ml of glacial acetic acid were added to the CIH solution and the pH was adjusted to 1.8.

Glutaraldehyde-fixed erythrocyte ghosts were spread flat at an air-water interface and mounted on collodion-coated (carbon-strengthened) electron microscope grids as described previously (25, 27). The mounted membranes were treated for 3 min with a 5% solution of bovine serum albumin (crystallized, Armour Pharmaceutical Co., Chicago, Ill.) in distilled water. Then the excess albumin was removed by touching the grids once to a drop of distilled water. Without drying, a large drop of the freshly prepared CIH solution was added to each of the grids at room temperature, and the staining was terminated after 2 min by quickly floating the CIH-treated grids on several large drops (five to six) of 12% acetic acid, pH 2.0, followed by distilled water (two). The total wash time never exceeded 1 min, including the two distilled water rinses. After removal of excess water with a filter paper, the grids were air dried before examination in a Hitachi Model HU-12 transmission electron microscope.

RESULTS

pH Effect

When unfixed human erythrocyte ghosts are suspended in low ionic strength buffers, their gross morphology is dependent on pH. Seen under phase contrast light microscopy, ghosts at pH 7.5 or 6.5 are smooth, round biconcave vesicles (Figs. 1 and 2); but as the pH is lowered to 5.5, the ghosts appear as irregularly shaped 'crumpled' vesicles (Fig. 3). At pH 4.5 two populations of ghosts are present: normal size 'smooth'-membrane ghosts and smaller 'rough'-membrane ghosts, accounting for approximately 10% and 90% of the ghost population respectively (Fig. 4). The morphology of the unfixed ghosts at pH 5.5 (crumpled) is reversible; that is, it can be reversibly changed from crumpled to smooth by increasing the pH. Either titrating the ghost suspension from pH 5.5 → 7.5 or resuspension in a pH 7.5 buffer changes ghost morphology back to the smooth shape (Fig. 5); however, reversibility is blocked by previous glutaraldehyde fixation at pH 5.5 (Fig. 6). Alternately, smooth ghosts prepared at pH 7.5 and fixed with glutaraldehyde, then shifted to pH 5.5, retain their smooth morphology characteristic of pH 7.5 (Fig. 7). These same membrane morphological states (smooth, crumpled, and rough) are easily recognizable in mounted unfixed or glutaraldehyde-fixed ghosts prepared for electron microscopy (Figs. 10–13).

When red cell ghosts, suspended in low ionic strength buffers for 5 min at pH 7.5, 6.5, 5.5, or 4.5 (followed by glutaraldhyde fixation), are mounted and labeled with CIH, different CIH topographical distributions are obtained. At pH 7.5 and 6.5 the bound CIH is found in small discrete clusters that are more or less randomly distributed on the ghost surface (Figs. 16 and 17). I will arbitrarily call this distribution the 'dispersed' state of CIH clusters, with the reminder that this will only be a working definition to describe obvious differences in the CIH-site topography. Ghosts suspended in low ionic strength buffers at pH 5.5 and fixed at pH 5.5 are obviously different in their CIH topography from ghosts fixed at pH 7.5 or 6.5—the CIH clusters are present in a more aggregated distribution (Fig. 18). The CIH distribution at pH 5.5 will arbitrarily be designated the 'aggregated' state to distinguish it from the CIH distributions obtained at pH 6.5 or 7.5. At pH 4.5 the dispersed (Fig. 19) and aggregated (Fig. 20) states are present on the smooth and rough ghosts, respectively. To test the reversibility of the CIH distributions at pH 7.5 and 5.5, ghosts were incubated at these pH values and then shifted (pH 7.5 → pH 5.5 and pH 5.5 → pH 7.5) for 5 min, followed by fixation. As before, the ghosts that were shifted pH 7.5 → 5.5 were crumpled in shape (Fig. 3) and had an aggregated CIH distribution (Fig. 21), while the ghosts that were shifted pH 5.5 → 7.5 were smooth (Fig. 5) and had a dispersed CIH distribution (Fig.

Figs. 1–9 are phase contrast photomicrographs of human erythrocyte ghosts. Bars equal 5 μm for Figs. 1–9. × 1,640.

FIGURE 1 Human erythrocyte ghosts incubated in 8 mM phosphate buffer at pH 7.5.

FIGURE 2 Legend is the same as in Fig. 1, except pH is 6.5.

FIGURE 3 Erythrocyte ghosts in 8 mM acetate buffer at pH 5.5.

FIGURE 4 Legend is the same as in Fig. 1, except pH is 4.5. Two types of ghosts are present, smooth (*s*) and rough (*r*).

FIGURE 5 Legend is the same as in Fig. 1, except that ghosts were first incubated in 8 mM acetate buffer, pH 5.5 and then shifted to 8 mM phosphate buffer pH 7.5.

FIGURE 6 Legend is the same as in Fig. 5, except that ghosts were fixed with glutaraldehyde in 8 mM acetate buffer at pH 5.5 and then shifted to phosphate buffer, pH 7.5.

FIGURE 7 Legend is the same as in Fig. 6, except that ghosts were fixed in phosphate buffer at pH 7.5, and then shifted to acetate buffer, pH 5.5.

FIGURE 8 Trypsinized human erythrocyte ghosts in phosphate buffer, pH 7.5.

FIGURE 9 Phospholipase C treated human erythrocyte ghosts in phosphate buffer, pH 7.5.

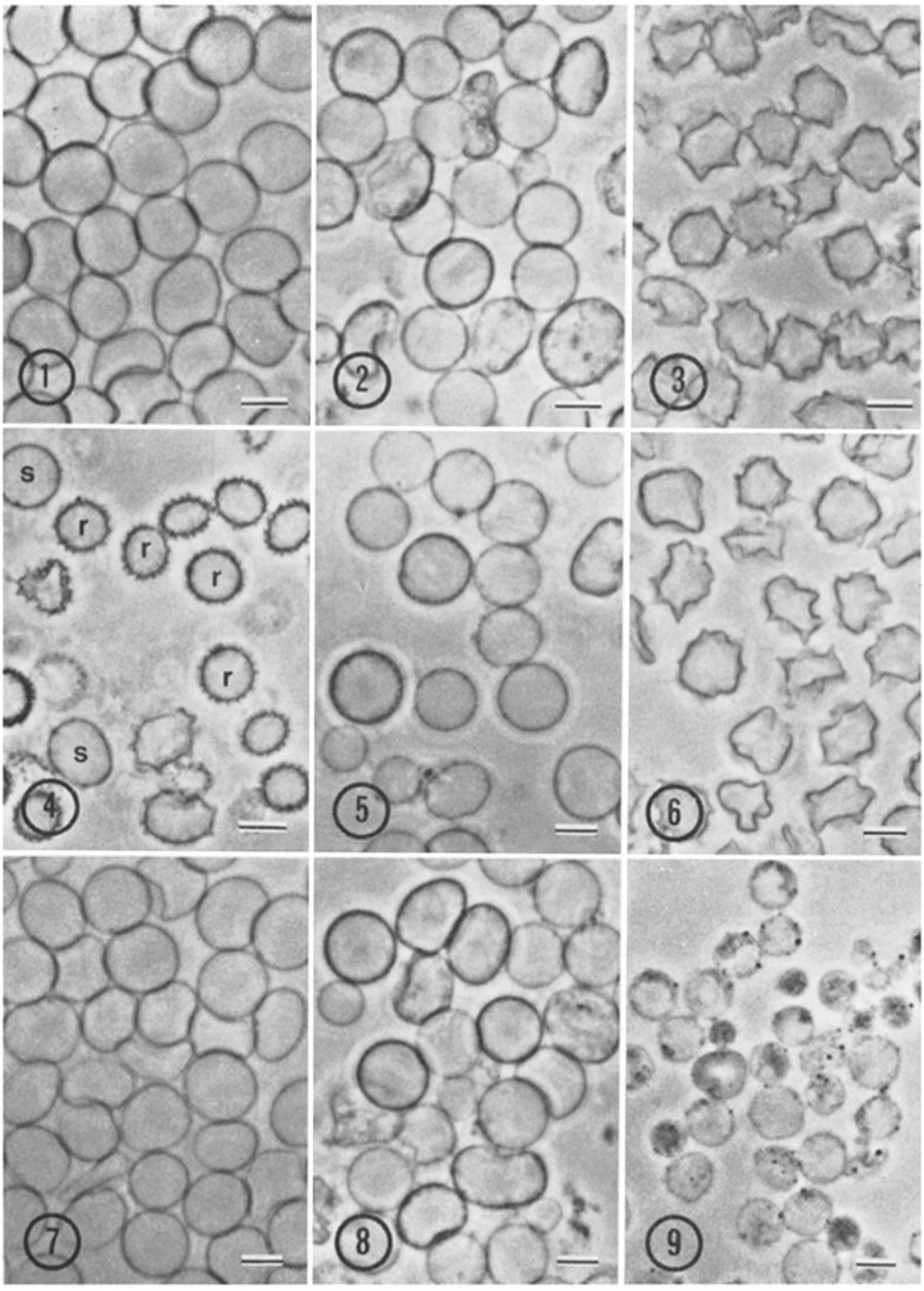
1
2
3
s
r
r
r
r
s
4
5
6
7
8
9

22). These experiments and their results are summarized in Table I.

Enzyme Effects

Treatment of human erythrocyte ghosts with crystalline trypsin at pH 7.5 did not cause gross morphological changes in ghost structure (Figs. 8, 14); that is, they remained normal in shape and their membranes remained smooth. However, the trypsin treatment causes a decrease in the total number of bound CIH particles and a shift to the aggregated CIH topographical state (Fig. 23). Previous fixation of ghosts in glutaraldehyde before trypsinization generally prevented aggregation of the CIH sites but did not prevent a reduction in the number of bound CIH particles (Fig. 24).

Phospholipase C treatment at pH 7.5, on the other hand, reduced the diameter of both unfixed and fixed ghosts seen under phase microscopy (Fig. 9) and fixed ghosts (fixed after PLC treatment) seen in electron micrographs (Fig. 15). Also, the smooth surface appearance was occasionally interrupted by small blebs or highly refractive zones on the ghost surface (Figs. 9 and 15). Examination of the membrane-bound CIH in electron micrographs of PLC-treated ghosts revealed a very aggregated CIH topographical distribution (Fig. 25).

Incubation of unfixed (or fixed) ghosts in a solution containing neuraminidase reduced the number of membrane-bound CIH particles to less than 10–15% of the control ghost preparations (Fig. 26).

DISCUSSION

CIH is bound to cell membranes by coulombic interaction with negatively charged surface groups (12, 13, 45, 47–49). At pH 1.8, where the staining reaction is performed, most anionic surface groups are uncharged, except acidic groups like NANA and its derivatives (12, 45, 47–49) (with a pK of approximately 2.7 NANA is partially charged at pH 1.8 [47]), sulfate (12, 13, 45, 48), and ribonucleic acid or phosphate (20, 45, 46). Since neuraminidase is able to specifically cleave greater than 90% of membrane-bound human erythrocyte NANA (see also references 11 and 49) and concurrently reduce CIH labeling to below 15% of the untreated controls, the CIH binding sites on fixed human red cells at pH 1.8 are predominantly the carboxyl groups of NANA. This conclusion was also arrived at by Weiss et al. (49). They used conventional plastic embedding of CIH-labeled control and neuraminidase-treated, intact glutaraldehyde-fixed human erythrocytes and found that the enzyme-treated cells bound less than 20% of the CIH compared to the untreated cells.

The topographic distribution of bound CIH on fixed human erythrocyte membrane surfaces is not periodic or uniform; the CIH particles are found in small randomly arranged clusters. These clusters contain several CIH particles, arranged occasionally in short linear arrays of a few hundred Ångstroms in length. These small CIH clusters could be artifacts of the glutaraldehyde fixation, since it is known that glutaraldehyde can affect membrane protein conformational stability as measured by circular dichroism (CD). For example, the CD spectra obtained after glutaraldehyde fixation of human erythrocyte ghosts indicate a slight loss of membrane protein helicity (16). Another explanation for the presence of small CIH clusters is that the clusters represent CIH binding to discrete membrane structures or groups of structures that contain greater than average densities of acidic residues (20, 48, 49). Recently, Marchesi and his collaborators (19) have described the characterization of a human red cell membrane sialoglycoprotein called *glycophorin* that is 60% carbohydrate and 40% protein in the form of a single polypeptide chain. Each molecule of *glycophorin* contains approximately 30 NANA residues at the termini of several oligosaccharide chains. These oligosaccharide chains also contain ABO blood group antigens, influenza virus, and phytohemagglutinin receptors. The saccharide chains are linked to a hydrophilic sequence of amino acids near the N-terminal end. This hydrophilic region of the polypeptide presumably rotates freely in the aqueous phase. The C-terminal region of the polypeptide chain is also hydrophilic, but a large internal region is hydrophobic in composition. Because of this hydrophobicity, the internal peptide sequence is probably buried in the membrane interior (37, 40, 50) providing a "membrane anchor" for this (amphipathic?) molecule. The saccharide containing N-terminal end of *glycophorin* may exist as a linear polymer without tertiary structure, maximizing distances between the NANA residues and binding several CIH particles at NANA residues on its

saccharide side chains. If this configuration is correct, then an almost linear-like array of CIH particles would not be unexpected (Fig. 27), especially if the glycopeptide chain collapses during dehydration as suggested by Parsons and Subjeck (32).

The morphology of human erythrocyte ghosts and the topographic distribution of CIH were

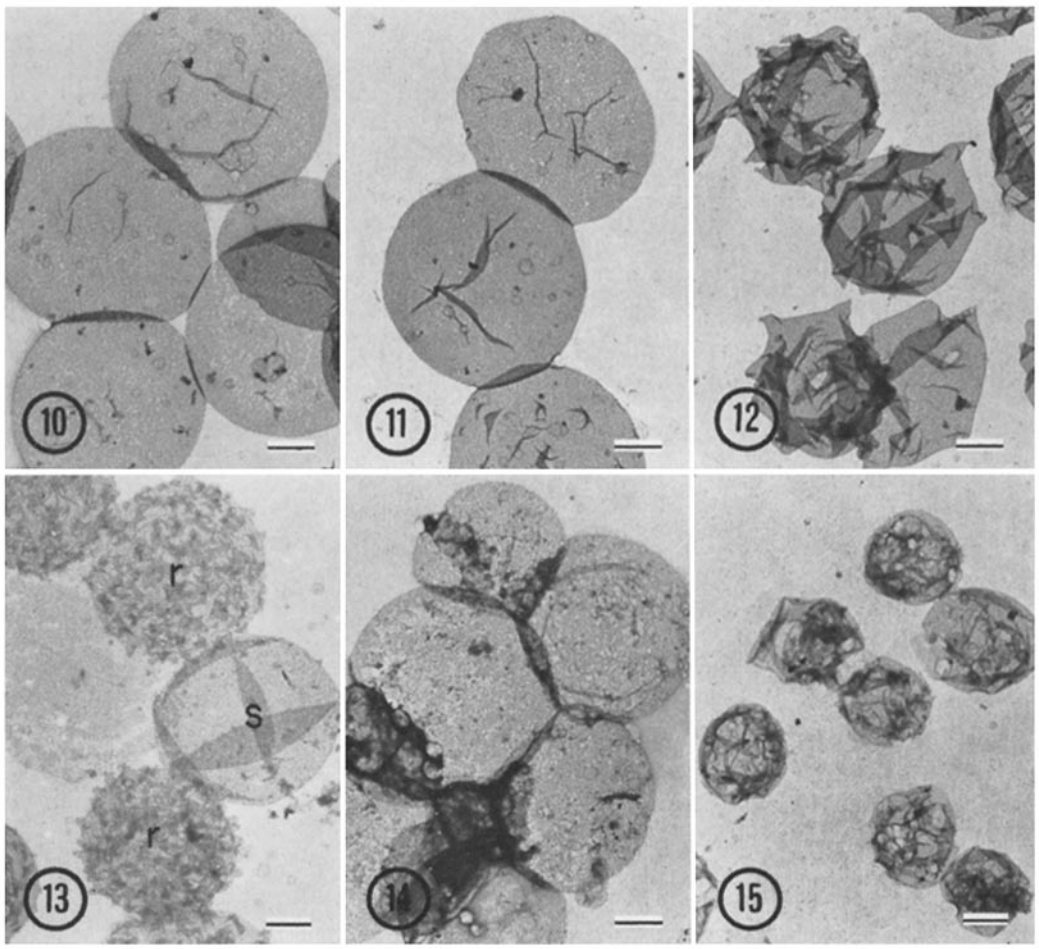

FIGS. 10–15 are electron micrographs of mounted unstained human erythrocyte ghosts. Bars equal 2 μm for Figs. 10–15. × 3,200.

FIGURE 10 Human erythrocyte ghosts incubated in 8 mM phosphate buffer, pH 7.5, fixed with glutaraldehyde, and mounted on a carbon-collodion coated grid without staining.

FIGURE 11 Legend is the same as in Fig. 10, except that the pH was 6.5 during the incubation and fixation.

FIGURE 12 Legend is the same as in Fig. 10, except that ghosts were incubated and fixed with glutaraldehyde in acetate buffer, pH 5.5.

FIGURE 13 Legend is the same as in Fig. 10, except that the pH was 4.5 during the incubation and fixation. Two types of ghosts are present, smooth (*s*) and rough (*r*).

FIGURE 14 Trypsinized ghosts in phosphate buffer pH 7.5 were fixed with glutaraldehyde and mounted on a carbon-collodion grid without staining.

FIGURE 15 Legend is the same as in Fig. 14, except the ghosts were treated with phospholipase C.

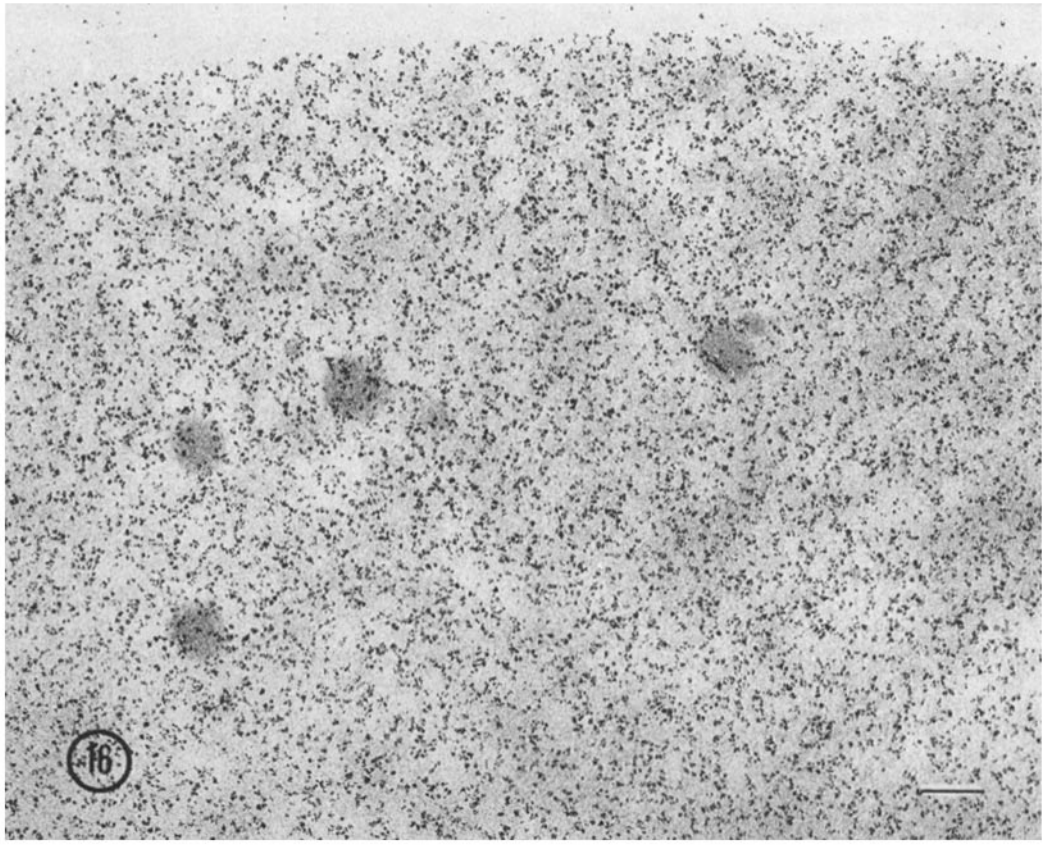

FIGURE 16 Topographic distribution of colloidal iron hydroxide on the surface of a glutaraldehyde-fixed human erythrocyte ghost. Ghosts were incubated in 8 mM phosphate buffer, pH 7.5, and fixed at pH 7.5 with glutaraldehyde. After fixation the ghosts were mounted on carbon-collodion films and directly stained with colloidal iron hydroxide. Bar equals 0.1 μm. × 82,000.

found to be sensitive to pH in low ionic strength buffers. At pH 6.5 or 7.5 the ghosts were smooth biconcave vesicles, and CIH was distributed in small randomly dispersed clusters. At pH 5.5 the ghost membranes appeared crumpled, and CIH was distributed in a more aggregated manner compared to the distribution at pH 7.5. When the pH was reduced to 4.5, two populations of ghosts were present: approximately 10% were smooth-shaped ghosts having a dispersed CIH distribution, and the remainder were very rough in shape with small villus-like structures and an aggregated CIH distribution. The morphology and aggregation of CIH particles at pH 5.5 were reversible; the crumpled ghosts could be transformed into smooth ghosts and the CIH distribution into a dispersed topography by suspending the ghosts at pH 7.5. That the ghost morphology and CIH distribution are artifacts of glutaraldehyde fixation and are not related directly to pH effects is ruled out by the following: (*a*) glutaraldehyde fixation did not affect ghost morphology under phase or electron microscopy, (*b*) ghosts in various pH buffers were fixed identically except for the pH during incubation and fixation, (*c*) glutaraldehyde fixation prevented pH-induced changes in morphology and CIH distribution, and (*d*) when unfixed membranes stained with ferritin-conjugated *Ricinus communis* agglutinin were examined, these same pH-induced topographical changes were found (G. L. Nicolson, unpublished observations). These results are similar to those of Pinto da Silva (33) where the distribution of the human erythrocyte intramembranous particles (34) revealed by freeze-cleavage was found to be sensitive to pH

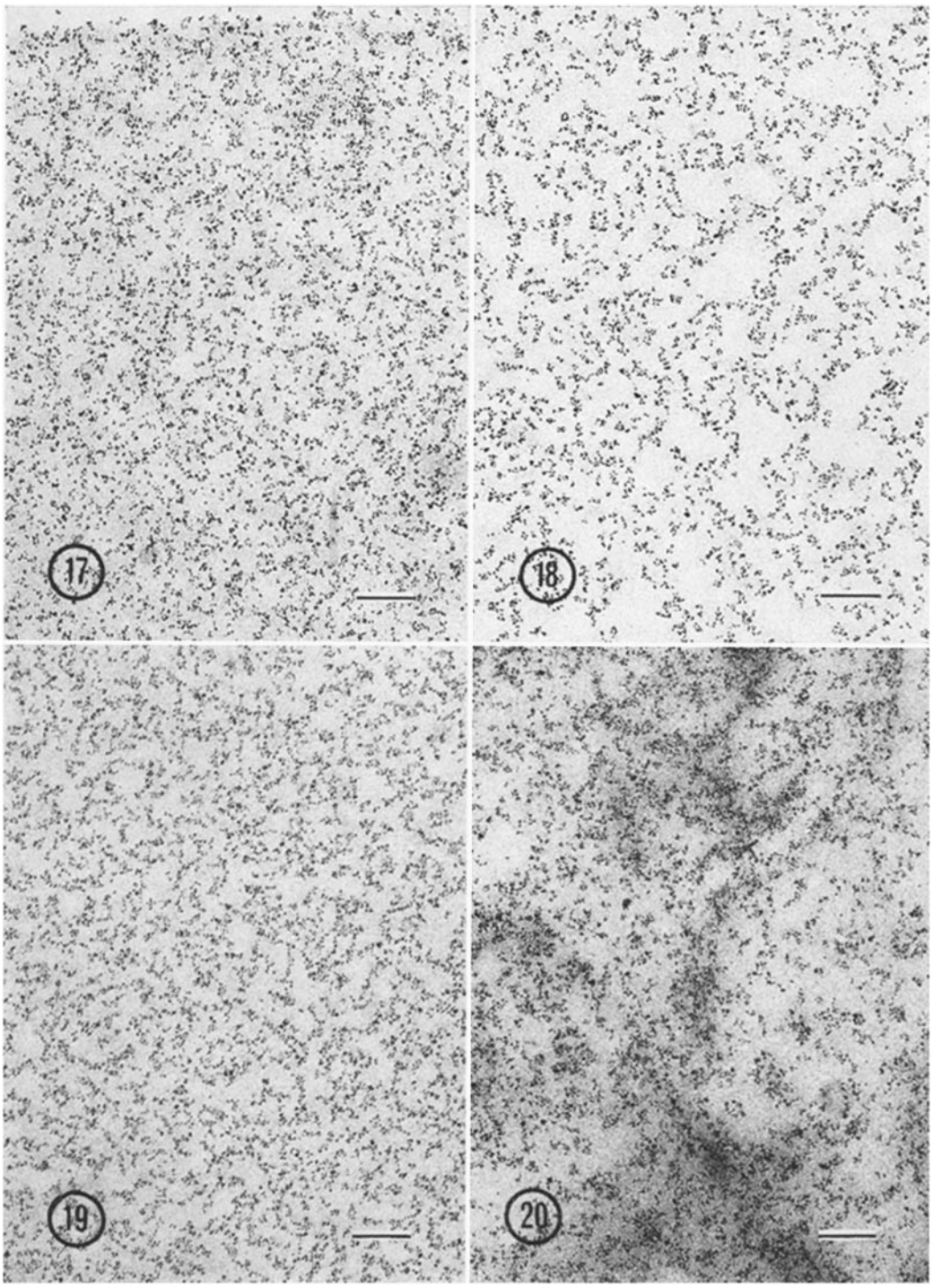

FIGURE 17 Legend is the same as in Fig. 16, except ghosts were incubated and fixed at pH 6.5. Bar equals 0.1 μm. × 82,000.

FIGURE 18 Legend is the same as in Fig. 16, except that ghosts were incubated and fixed in acetate buffer, pH 5.5. Bar equals 0.1 μm. × 82,000.

FIGURE 19 Legend is the same as in Fig. 16, except that ghosts were incubated and fixed at pH 4.5. The colloidal iron hydroxide distribution on a smooth ghost is shown here. Bar equals 0.1 μm. × 82,000.

FIGURE 20 Legend is the same as in Fig. 19, except that the colloidal iron hydroxide distribution is that of a rough ghost. Bar equals 0.1 μm. × 82,000.

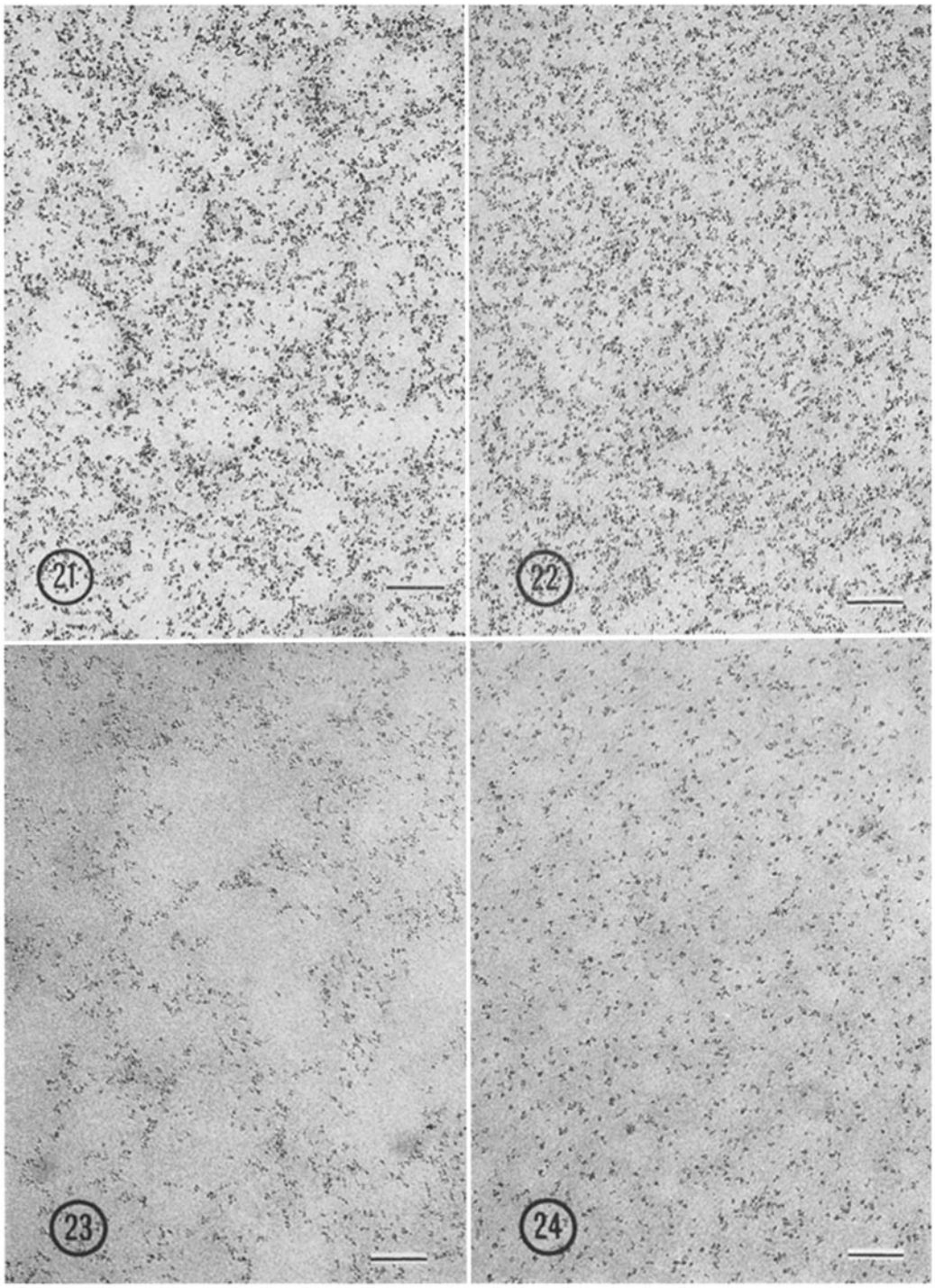

FIGURE 21 Legend is the same as in Fig. 16, except that ghosts were incubated in phosphate buffer, pH 7.5, and then shifted to acetate buffer, pH 5.5, and fixed with glutaraldehyde. Bar equals 0.1 μm. × 82,000.

FIGURE 22 Legend is the same as in Fig. 16, except that ghosts were incubated in acetate buffer, pH 5.5, and then shifted to phosphate buffer, pH 7.5, and fixed with glutaraldehyde. Bar equals 0.1 μm. × 82,000.

FIGURE 23 Legend is the same as in Fig. 16, except that ghosts were treated with trypsin before fixation. Bar equals 0.1 μm. × 82,000.

FIGURE 24 Legend is the same as in Fig. 23, except that ghosts were fixed with glutaraldehyde before trypsinization. Bar equals 0.1 μm. × 82,000.

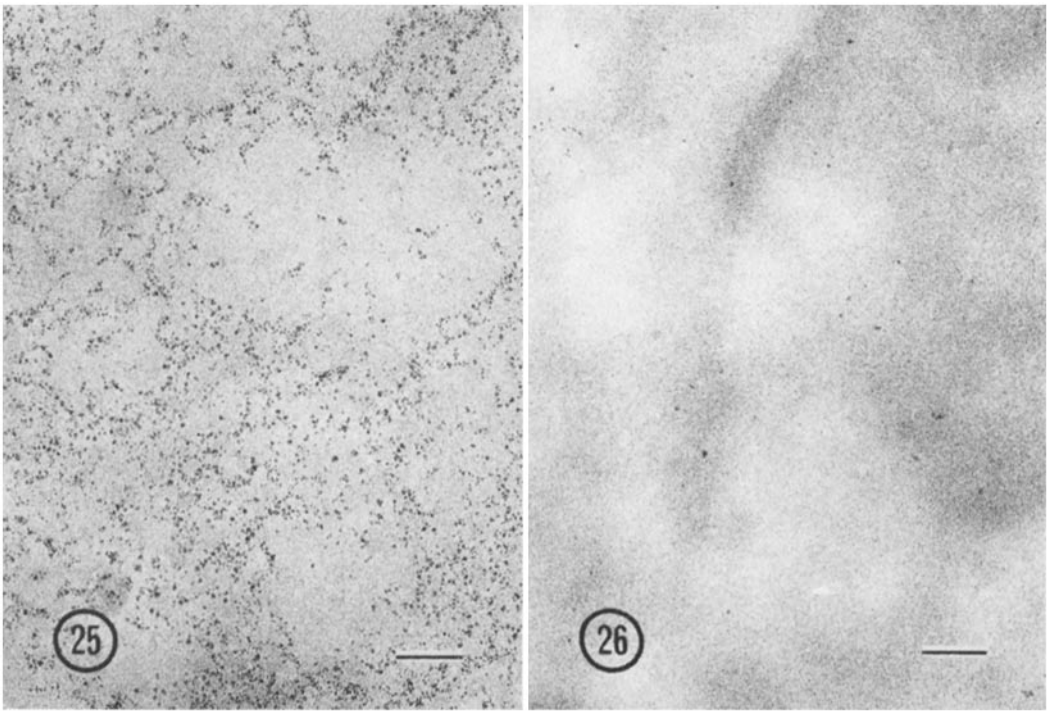

FIGURE 25 Topographic distribution of colloidal iron hydroxide on the surface of a phospholipase C treated human erythrocyte ghost. Bar equals 0.1 μm. × 82,000.

FIGURE 26 Legend is the same as in Fig. 23, except that ghosts were treated with neuraminidase. Bar equals 0.1 μm. × 82,000.

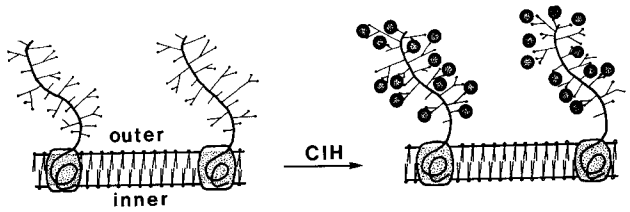

FIGURE 27 A proposal for the binding of colloidal iron hydroxide to *glycophorin* *N*-acetylneuraminic acid residues on the surface of human erythrocyte membranes. The *glycophorin* model has been adapted from Marchesi, et al. (19), Tillack, et al. (40), and Winzler (50). *Inner*, inner cytoplasmic surface of erythrocyte membrane; *outer*, outer extracellular surface of erythrocyte membrane; *CIH*, colloidal iron hydroxide.

at low ionic strength. The intramembranous particles were in a dispersed state at pH 7.5 to 9.5 and at pH 4.5, but were aggregated at pH 4.8 to 5.5 and at or below pH 3.5. It was also found that previous glutaraldehyde fixation at pH 7.5 prevented particle aggregation at pH 5.5 and that high ionic buffers also prevented aggregation (33).

The relationship of the intramembranous particles of human erythrocytes to known membrane components has been established by freeze-etching experiments (35, 40). After purposely aggregating the intramembranous particles, ghosts were labeled with markers such as ferritin-conjugated antibodies, ferritin-conjugated plant agglutinins, or *influenza* virus particles and were then freeze-cleaved followed by brief etching to reveal the outer membrane surface. On the etched surfaces the markers for ABO antigens (35), phytohemagglutinin sites, and virus receptors (40) were

distributed in aggregated distributions similar to the intramembranous particles, and where the etched surface met the fracture plane the markers were contiguous with the intramembranous particles. Since human erythrocyte *glycophorin* contains ABO antigens, phytohemagglutinin and influenza receptors, and also approximately 80% of the membrane associated NANA (19), it seems likely that the freeze-cleavage experiments (33) and the CIH-labeling experiments presented here have determined the topography of the same membrane component(s) by different means.

The data of Pinto da Silva (33) differ slightly from mine in two respects. First, it was not reported that two morphological types of membranes were obtained at pH 4.5. This could be explained by possible difficulties in obtaining adequate fracture faces from the rough surfaced ghost population. Here it was found that this population accounted for approximately 90% of the ghosts and had an aggregated CIH distribution. Second, the percent recovery for ghosts undergoing pH-induced changes in morphology and CIH distribution was never 100%. In experiments where the pH was shifted 7.5 → 5.5 → 7.5 → 5.5 → 7.5, the yield of ghosts with normal pH 7.5 morphology and CIH distribution was approximately 70–90%. The reason(s) for nonquantitative pH-induced transition is not clear, but one possibility is that repeated centrifugation during the washing steps in low ionic strength buffers damaged some of the ghosts.

Proteolysis of intact cells has been extensively used to increase the reactiveness of membrane antigen (15) and lectin (7, 8) sites as monitored by cell agglutination. It has been demonstrated recently that the increased agglutinability of proteolytic enzyme-treated cells with concanavalin A (Con A) is not due to an increase in the number of membrane-binding sites (31), but rather it is due to a change in the distribution of membrane Con A sites to a more clustered configuration that favors cell agglutination (23, 24). The distribution of CIH sites is modified in a similar manner; that is, the small CIH clusters are found in a highly aggregated state after trypsinization. Other proteases (pronase, papain, and ficin) similarly modify the topography of CIH sites and also Con A and *Ricinus communis* sites on human erythrocytes (reference 23 and G. L. Nicolson, unpublished data). The intramembranous freeze-etch particles are also known to be nonreversibly aggregated by proteolysis under similar conditions required to aggregate the CIH sites (10, 40).

There is good evidence that proteolysis of erythrocyte ghosts results in release of peptides containing NANA (38, 51). Steck et al. (38) and Triplett and Carraway (41) have shown that the sialoglycoprotein of human erythrocytes can be destroyed by extensive protease digestion. This can be interpreted as evidence that mild proteolysis has a direct effect on the CIH-binding glycopeptides; that is, their partial removal results in aggregation of the remaining CIH sites along with the aggregation of lectin sites and the freeze-etch intramembranous particles. Since proteolysis removes membrane NANA, the aggregation of the remaining CIH sites appears to involve electrostatic effects (33).

PLC treatment causes intense aggregation of the CIH sites in an analogous fashion to trypsinization. The effects of PLC on erythrocyte ghosts has been well studied by Ottolenghi and his collaborators (4, 30). PLC specifically cleaves organophosphorous compounds from membrane phospholipids (29). The phosphorus compounds (phosphocholine, phosphoethanolamine, etc.) are solubilized while the diglyceride remains membrane-bound and probably pools by diffusion to form the membrane "blebs" (3, 30). The blebs have been found to contain myelin figures after osmium fixation (30) and do not appear to contain agglutinin sites (reference 24 and G. L. Nicolson, unpublished observations) or intramembranous particles (42). These observations suggest that PLC causes aggregation by perturbing membrane lipid charge or lipid-protein interactions, or both. The membrane protein conformation does not appear to be greatly affected by PLC, as indicated by CD (14) and spin-label studies (35A). Thus, the CIH sites present on saccharide chains can be affected by events occurring at the immediate membrane surface and/or below the membrane surface in the hydrophobic domain.

The most probable explanation for the reversible changes in CIH-site distribution is that the CIH binding sites are present on intrinsic membrane molecules that are capable of translational diffusion in the membrane plane. There is now good evidence for a fluid dynamic structure of membranes (37), one that permits lateral diffusion of membrane intrinsic components but also follows certain necessary thermodynamic restraints (36). The pH and proteolysis experiments suggest that

the distribution of the CIH sites is dependent on electrostatic events while the lipase experiments suggest that it may also be determined by interactions in the membrane hydrophobic domain. The identification of acidic residues on the N-terminal hydrophilic region of *glycophorin*, its close identification with the intramembranous particles, and the demonstration by Bretscher (5) that this molecule can be labeled from either side of the ghost membrane by a reagent that has low penetrability in the membrane hydrophobic regions (6) indicates that events (*a*) on the membrane exterior surface, (*b*) in the membrane hydrophobic domain, and (*c*) on the membrane interior surface may determine the topographic distribution of (*glycophorin*) CIH sites. For example, an explanation for the aggregation of CIH sites at pH 5.5 might follow from case *c*, above. Spectrin (18), a fibrous protein that is located on the interior surface of human erythrocyte ghosts (26), has an isoelectric point around pH 5.5 (V. T. Marchesi, personal communication). If spectrin molecules are physically interacting with *glycophorin* molecules, an isoelectric aggregation of spectrin might cause a similar, but indirect, effect on *glycophorin* and its CIH-binding NANA residues. A possible experiment to test this hypothesis might be to sequester antispectrin immunoglobulin molecules inside the ghosts during the hemolysis steps. If spectrin is in fact involved in the aggregation of *glycophorin* at pH 5.5, antispectrin might be able to aggregate spectrin molecules on the interior membrane surface at pH 7.5 similar to the antibody-induced aggregation of antigenic sites on the exterior surface of lymphoid cells (39). Determining the distribution of CIH sites or intramembranous particles after antispectrin treatment should provide a means to eliminate this possibility.

I would like to thank Miss Monique Lacorbiere and Mr. Peter Delmonte for their excellent technical assistance.

This investigation was supported by a grant (GE-34178) from the Human Cell Biology Program of the National Science Foundation, a contract (72-3207) from the Special Virus-Cancer Program of the National Cancer Institute, United States Public Health Service, and grants from the New York Cancer Research Institute and the Armand Hammer Fund for Cancer Research.

Received for publication 18 September 1972, and in revised form 16 November 1972.

Note Added in Proof: We have recently found that sequestering antispectrin γG molecules inside washed human ghosts during hemolysis leads to aggregation of CIH sites on the exterior membrane surface. The antispectrin-induced aggregation is a time-, temperature-, and concentration-dependent process and requires cross-linking γG molecules. Sequestered univalent antispectrin Fab molecules have no effect on CIH site distribution. Also, previous glutaraldehyde fixation prevents antispectrin γG-induced aggregation (G. L. Nicolson and R. Painter, in preparation). This finding is probably an example of *trans*-membrane (see reference 37) control of the erythrocyte surface through integral membrane components that span the membrane. Similar macromolecular structures in other cell membranes may provide the means by which cells can exert cytoplasmic control over their shape and spatial organization of surface components.

REFERENCES

1. AMBROSE, E. J. 1966. Electrokinetic behavior of cells. *Prog. Biophys. Mol. Biol.* **16**:241.
2. BARTLETT, G. R. 1969. Phosphorus assay in column chromatography. *J. Biol. Chem.* **234**:466.
3. BENEDETTI, E. L., and P. EMMELOT. 1966. Ultrastructure of plasma membranes after phospholipase C treatment. *J. Microsc. (Paris).* **5**:645.
4. BOWMAN, M. H., A. C. OTTOLENGHI, and C. E. MENGEL. 1971. Effects of phospholipase C on human erythrocytes. *J. Membrane Biol.* **4**:156.
5. BRETSCHER, M. S. 1971. A major protein which spans the human erythrocyte membrane. *J. Mol. Biol.* **59**:351.
6. BRETSCHER, M. S. 1971. Human erythrocyte membranes: specific labeling of surface proteins. *J. Mol. Biol.* **58**:775.
7. BURGER, M. M., and A. R. GOLDBERG. 1967. Identification of a tumor-specific determinant on neoplastic cell surfaces. *Proc. Natl. Acad. Sci. U. S. A.* **57**:359.
8. BURGER, M. M. 1969. A difference in the architecture of the surface membrane of normal and virally transformed cells. *Proc. Natl. Acad. Sci. U. S. A.* **62**:1074.
9. DODGE, J. T., C. MITCHELL, and D. J. HANAHAN. 1963. The preparation and chemical characteristics of hemoglobin-free ghosts of human erythrocytes. *Arch. Biochem. Biophys.* **100**:119.
10. ENGSTRÖM, L. 1970. Structure in the Erythrocyte Membrane. Ph.D. Dissertation. University of California, Berkeley.

11. EYLAR, E. H., M. A. MADOFF, O. V. BRODY, and J. L. ONCLEY. 1962. The contribution of sialic acid to the surface charge of the erythrocyte. *J. Biol. Chem.* **237**:1992.
12. GASIC, G., and L. BERWICK. 1963. Hale stain for sialic acid-containing mucins. Adaption to electron microscopy. *J. Cell Biol.* **19**:223.
13. GASIC, G. J., L. BERWICK, and M. SORRENTINO. 1968. Positive and negative colloidal iron as cell surface electron stains. *Lab. Invest.* **18**:63.
14. GLASER, M., H. SIMKINS, S. J. SINGER, M. SHEETZ, and S. I. CHAN. 1970. On the interactions of lipids and proteins in the red blood cell membrane. *Proc. Natl. Acad. Sci. U. S. A.* **65**:721.
15. KABAT, E. A. 1956. *In* Blood Group Substances. Their Chemistry and Immunochemistry. Academic Press Inc., New York. 47.
16. LENARD, J., and S. J. SINGER. 1968. Alteration of proteins in red blood cell membranes and in solution by fixatives used in electron microscopy. *J. Cell Biol.* **37**:117.
17. LENARD, J., and S. J. SINGER. 1968. Reaction of red blood cell membranes with phospholipase C. *Science (Wash. D. C.).* **159**:738.
18. MARCHESI, V. T., E. STEERS, T. W. TILLACK, and S. L. MARCHESI. 1969. Some properties of spectrin. A fibrous protein isolated from red cell membranes. *In* The Red Cell Membrane, Structure and Function. G. A. Jamieson and T. J. Greenwald, editors. J. B. Lippincott Company, Philadelphia. 117.
19. MARCHESI, V. T., T. W. TILLACK, R. L. JACKSON, J. P. SEGREST, and R. E. SCOTT. 1972. Chemical characterization and surface orientation of the major glycoprotein of the human erythrocyte membrane. *Proc. Natl. Acad. Sci. U. S. A.* **69**:1445.
20. MEHRISHI, J. N. 1972. Surface molecular components of Ehrlich ascites tumour cells. *Blut Z. Gesamte Blutforsch.* **24**:388.
21. NICOLSON, G. L. 1971. Difference in topology of normal and tumor cell membranes as shown by different surface distributions of ferritin-conjugated concanavalin A. *Nat. New Biol.* **233**:244.
22. NICOLSON, G. L. 1972. A rapid method for determining the topological distribution of anionic sites on membrane surfaces. *J. Supramolecular Struct.* **1**:159.
23. NICOLSON, G. L. 1972. Topological studies on the structure of cell membranes. *In* Membrane Research: Proceedings of the 1972 California Membrane Conference. C. F. Fox, editor. Academic Press Inc., New York. 53.
24. NICOLSON, G. L. 1972. Topography of membrane concanavalin A sites modified by proteolysis. *Nat. New Biol.* **239**:193.
25. NICOLSON, G. L., R. HYMAN, and S. J. SINGER. 1971. The two-dimensional topographic distribution of H-2 histocompatibility alloantigens on mouse red blood cell membranes. *J. Cell Biol.* **50**:905.
26. NICOLSON, G. L., V. T. MARCHESI, and S. J. SINGER. 1971. The localization of spectrin on the inner surface of human red blood cell membranes by ferritin-conjugated antibodies. *J. Cell Biol.* **51**:265.
27. NICOLSON, G. L., and S. J. SINGER. 1971. Ferritin conjugated plant agglutinins as specific saccharide stains for electron microscopy: Application to saccharides bound to cell membranes. *Proc. Natl. Acad. Sci. U. S. A.* **68**:942.
28. OHTA, N., A. B. PARDEE, B. R. MCAUSLAN, and M. M. BURGER. 1968. Similar sialic acid contents and controls of normal and malignant cells. *Biochim. Biophys. Acta.* **158**:98.
29. OTTOLENGHI, A. C. 1965. Phospholipase C from *B. cereus*, a zinc-requiring metaloenzyme. *Biochim. Biophys. Acta.* **106**:510.
30. OTTOLENGHI, A. C., and M. H. BOWMAN. 1970. Membrane structure: Morphological and chemical alterations in phospholipase C-treated mitochondria and red cell ghosts. *J. Membrane Biol.* **2**:180.
31. OZANNE, B., and J. SAMBROOK. 1971. Binding of radioactively labeled concanavalin A and wheat germ agglutinin to normal and virus-transformed cells. *Nat. New Biol.* **232**:156.
32. PARSONS, D. F., and J. R. SUBJECK. 1972. The morphology of the polysaccharide coat of mammalian cells. *Biochim. Biophys. Acta.* **265**:85.
33. PINTO DA SILVA, P. 1972. Transitional mobility of the membrane intercalated particles of human erythrocyte ghosts. pH-dependent, reversible aggregation. *J. Cell Biol.* **53**:777.
34. PINTO DA SILVA, P., and D. BRANTON. 1970. Membrane splitting in freeze-etching. Covalently bound ferritin as a membrane marker. *J. Cell Biol.* **45**:598.
35. PINTO DA SILVA, P., D. BRANTON, and S. D. DOUGLAS. 1971. Localization of A_1 antigen sites on human erythrocyte ghosts. *Nature (Lond.).* **232**:194.
35A. SIMKINS, H., E. PANKO, and S. TAY. 1971. Evidence that suggests the existence of lipid regions discrete from those of the protein in mitochondrial and red blood cell membranes. *J. Membrane Biol.* **5**:334.
36. SINGER, S. J. 1971. The molecular organization of biological membranes. *In* Structure and Function of Biological Membranes. L. I.

Rothfield, editor. Academic Press Inc., New York. 145.

37. SINGER, S. J., and G. L. NICOLSON. 1972. The fluid mosaic model of the structure of cell membranes. *Science (Wash. D. C.)*. **175**:720.
38. STECK, T. L., G. FAIRBANKS, and D. F. Hr WALLACH. 1971. Disposition of the majo' proteins in the isolated erythrocyte membrane. Proteolytic dissection. *Biochemistry*. **10**:2617.
39. TAYLOR, R. G., P. H. DUFFUS, M. C. RAFF, and S. DE PETRIS. 1971. Redistribution and pinocytosis of lymphocyte surface immunoglobulin molecules induced by anti-immunoglobulin antibody. *Nat. New Biol.* **233**:225.
40. TILLACK, T. W., R. E. SCOTT, and V. T. MARCHESI. 1972. The structure of erythrocyte membranes studied by freeze-etching. II. Localization of the receptors for phytohemagglutinin and *influenza* virus to the intramembranous particles. *J. Exp. Med.* **135**:1209.
41. TRIPLETT, R. B., and K. L. CARRAWAY. 1972. Proteolytic digestion of erythrocytes, resealed ghosts and isolated membranes. *Biochemistry*. **11**:2897.
42. WALLACH, D. F. H. 1969. Membrane lipids and the conformations of membrane proteins. *J. Gen. Physiol.* **54**:35.
43. WARREN, L. 1959. The thiobarbituric acid assay of sialic acids. *J. Biol. Chem.* **234**:1971.
44. WEISS, L. 1969. The cell periphery. *Int. Rev. Cytol.* **26**:63.
45. WEISS, L., O. S. JUNG, and R. ZEIGEL. 1972. The topography of some anionic sites at the surfaces of fixed Ehrlich ascites tumor cells. *Int. J. Cancer*. **9**:48.
46. WEISS, L., and E. MAYHEW. 1969. Ribonuclease-susceptible charged groups at the surface of Ehrlich ascites tumor cells. *Int. J. Cancer*. **4**:626.
47. WEISS, L., and R. ZEIGEL. 1969. Cell surface negativity and the binding of positively charged particles. *J. Cell Physiol.* **77**:179.
48. WEISS, L., and R. ZEIGEL. 1972. Hetererogeneity of anionic sites at the electrokinetic surfaces of fixed Ehrlich ascites tumor cells. *J. Theor. Biol.* **34**:21.
49. WEISS, L., R. ZEIGEL, O. S. JUNG, and I. D. J. BROSS. 1972. Binding of positively charged particles to glutaraldehyde-fixed human erythrocytes. *Exp. Cell Res.* **70**:57.
50. WINZLER, R. J. 1970. Carbohydrates in cell surfaces. *Int. Rev. Cytol.* **29**:77.
51. WINZLER, R. J., E. D. HARRIS, D. J. PEKAS, D. A. JOHNSON, and P. WEBER. 1967. Studies on the glycopeptides released by trypsin from intact human erythrocytes. *Biochemistry*. **7**:2195.
52. WU, H. C., E. MEEZAN, P. H. BLACK, and P. W. ROBBINS. 1969. Comparative studies on the carbohydrate-containing membrane components of normal and virus-transformed mouse fibroblasts. I. Glucosamine-labeling patterns in 3T3, spontaneously transformed 3T3 and SV40-transformed 3T3 cells. *Biochemistry*. **8**:2509.